

Amphiregulin Promotes Resistance to Gefitinib in NonSmall Cell Lung Cancer Cells by Regulating Ku70 Acetylation

Benoît Busser¹⁻³, Lucie Sancey^{1,2}, Véronique Josserand^{1,2}, Carole Niang^{1,2}, Saadi Khochbin^{1,2}, Marie C Favrot¹⁻³, Jean-Luc Coll^{1,2} and Amandine Hurbin^{1,2}

¹INSERM, U823, Institut Albert Bonniot, Grenoble, France; ²Université Joseph Fourier, Grenoble, France; ³CHRU Grenoble, Hôpital Michallon, UF Cancérologie Biologique et Biothérapie, Grenoble, France

Multiple molecular resistance mechanisms reduce the efficiency of receptor tyrosine kinase inhibitors such as gefitinib in non-small cell lung cancer (NSCLC). We previously demonstrated that amphiregulin (Areg) inhibits gefitinib-induced apoptosis in NSCLC cells by inactivating the proapoptotic protein BAX. In this part of the investigation, we studied the molecular mechanisms leading to BAX inactivation. We show that Areg prevents gefitinib-mediated acetylation of Ku70. This augments the BAX-Ku70 interaction and therefore prevents BAX-mediated apoptosis. Accordingly, Areg or Ku70 knock down restore BAX activation and apoptosis in gefitinib-treated H358 cells *in vitro*. In addition, overexpression of the histone acetyltransferase (HAT) CREB-binding protein (CBP) or treatments with histone deacetylase (HDAC) inhibitors sensitize H358 cells to gefitinib. Moreover, a treatment with vorinostat, a HDAC inhibitor strongly sensitized tumors to gefitinib *in vivo*. These findings suggest new prospects in combining both HDAC and epidermal growth factor receptor inhibitors for the treatment of NSCLC.

Received 20 March 2009; accepted 9 September 2009; published online 13 October 2009. doi:10.1038/mt.2009.227

INTRODUCTION

Epidermal growth factor receptor (EGFR) is frequently overexpressed in non-small cell lung cancers (NSCLC) and correlates with a poor clinical outcome.^{1,2} Inhibitors of the tyrosine kinase activity of EGFR (the EGFR-TKI family) were therefore developed. Small molecules that block the adenosine triphosphate binding site of the cytoplasmic domain of EGFR, such as gefitinib or erlotinib, showed potent antitumor activity against previously treated NSCLC.^{3,4} However, the limited response rates of patients to EGFR-TKI⁵ led to investigating the mechanisms leading to resistance to EGFR-TKI treatments.

The level of expression of the EGFR ligand amphiregulin (Areg) was correlated with a poor response to gefitinib.⁶ Areg is associated with shortened survival of patients with NSCLC

and poor prognosis.⁷ Our group previously reported that Areg inactivates the proapoptotic protein BAX⁸ and inhibits gefitinib-induced apoptosis in NSCLC.⁹ However, the molecular mechanisms governing Areg- and gefitinib-mediated BAX inactivation in NSCLC cells are still unknown.

Following its activation, BAX translocates from the cytosol to the outer mitochondrial membrane where it oligomerizes, rendering the membrane permeable, and allowing the release of several mitochondrial death-promoting factors.¹⁰ The Ku70 DNA end-joining protein has recently been shown to suppress apoptosis by sequestering BAX from the mitochondria.^{11,12} In contrast, when Ku70 is acetylated, it releases BAX, allowing it to translocate to the mitochondria and trigger cytochrome c release, leading to caspase-dependent death. Ku70 was first characterized as part of the Ku70/Ku80 heterodimer that is essential for the repair of DNA double-strand breaks by nonhomologous end joining and the rearrangement of antibody and T cell receptor genes via V(D)J recombination,¹³ telomere maintenance and transcriptional regulation.¹⁴ Ku70 activity could be determined by its acetylation status, like other nonhistone proteins such as p53 and Hsp90.¹⁵ The acetylation level is regulated by both histone acetyltransferase (HAT) and histone deacetylase (HDAC) activities. Recent reports suggest that there is a positive relationship between Ku70 and the development of cancer, presenting Ku70 as an important target for anticancer drug development.¹²

In this study, we investigated the role of Ku70 in the Areg-regulated activity of gefitinib. We show that Areg inhibits apoptosis normally induced by gefitinib by an acetylation-dependent pathway leading to BAX inactivation. Areg reduces the acetylation of the protein Ku70 and thus enhances BAX inactivation. Consequently, enhancing acetylation abolishes the protective effect of Areg and renders NSCLC cells more sensitive to gefitinib treatment *in vitro* and *in vivo*.

RESULTS

Areg and Ku70 inhibit gefitinib-induced apoptosis in H358 NSCLC cells

H358 NSCLC cells overexpress Areg.¹⁶ Transfection of H358 cells with anti-Areg small-interfering RNAs (Areg siRNAs) strongly

reduced the secreted levels of Areg, as compared to control siRNAs, 3 and 4 days after transfection (Figure 1a). In addition, as shown in Figure 1b, Ku70 siRNA transfection considerably silenced the endogenous Ku70 in H358 cells. Interestingly, although anti-Areg or anti-Ku70 siRNA transfection did not induce apoptosis, it significantly sensitized H358 cells to 0.5 $\mu\text{mol/l}$ gefitinib (Figure 1c), suggesting that both Areg and Ku70 can reduce gefitinib efficiency. In addition, we verified that the Ku70 expression level was not modified by gefitinib and/or Areg treatments in the H358 cell line (data not shown). This indicated that Ku70 protein levels did not fluctuate with the Areg/ gefitinib cross-talk.

Areg and Ku70 inhibit BAX conformational change

We then investigated the relationship between gefitinib activity, Areg, Ku70, and BAX activation in H358 cells. We analyzed BAX activation by flow cytometry using an antibody that recognizes the exposed N-terminus of activated BAX but not the protein in its inactive conformation.¹⁷ The intensity of BAX immunostaining (Figure 2a, upper panel) as well as the percentage of positively stained cells (Figure 2b) were not modified by the gefitinib treatment, showing that BAX is not activated in these conditions. In addition, Areg or Ku70 knock down had a limited influence on BAX activation, because the exposure of its N-terminus moiety was not modified. In sharp contrast,

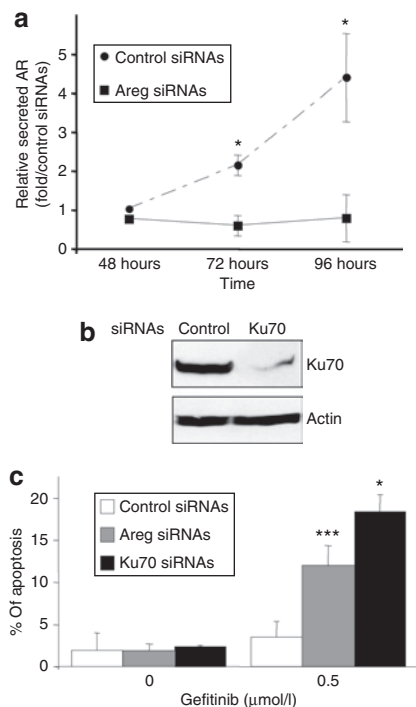


Figure 1 Areg and Ku70 inhibit gefitinib-induced apoptosis. H358 cells were transfected with control or amphiregulin (Areg) or Ku70 small-interfering RNAs (siRNAs) and treated with 0.5 $\mu\text{mol/l}$ gefitinib. (a) The efficiency of Areg knock down was assessed by enzyme-linked immunosorbent assay. Results are expressed as a rate of Areg released 48–96 hours after control siRNAs transfection and as mean \pm SD ($n = 3$). (b) The efficiency of Ku70 knock down was assessed after 96 hours by western blotting using Ku70 antibody. (c) Apoptosis was scored after counting Hoechst stained cells. Results are expressed as mean \pm SD ($n \geq 3$). * $P < 0.05$, *** $P < 0.001$, for comparison between treated and control cells.

cotreatment of the cells by Areg siRNAs (Figure 2a middle panel and Figure 2b) or Ku70 siRNAs (Figure 2a lower panel and Figure 2b) and gefitinib was associated with an activation of BAX. These data suggested that both Areg and Ku70 prevent BAX conformational activation, therefore inhibiting gefitinib activity.

Areg increases BAX/Ku70 interaction

To further demonstrate the role of Ku70 on Areg-dependent BAX inactivation, we measured the interaction between BAX and Ku70 using coimmunoprecipitation assays. We observed a low basal interaction between BAX and Ku70 in control H358

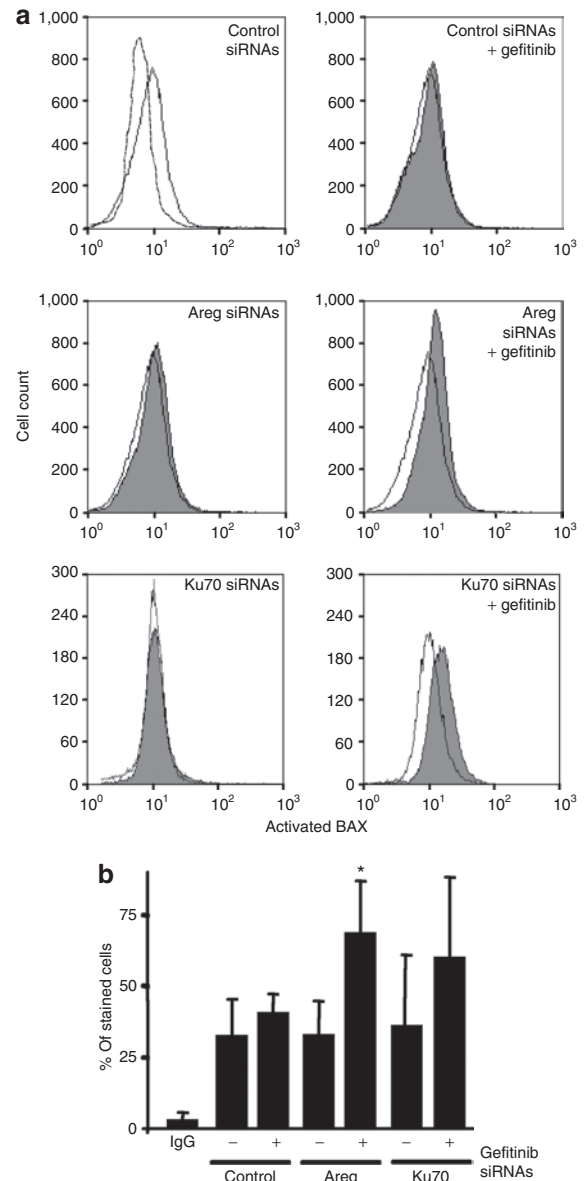


Figure 2 Areg and Ku70 inactivate BAX in H358 cells. H358 cells were transfected with control or amphiregulin (Areg) or Ku70 small-interfering RNAs and/or treated with 0.5 $\mu\text{mol/l}$ gefitinib. (a) Flow cytometry analysis of BAX immunostaining using activated-BAX antibody. Dotted histogram, irrelevant antibody; open histogram, control cells; filled histogram, treated cells as indicated. (b) Percentages of activated-BAX stained cells were expressed as mean \pm SD ($n \geq 3$). * $P < 0.05$, more significant than control.

cells (Figure 3a), which was enhanced under gefitinib treatment but only in the presence of Areg. Areg knock down significantly prevented this increase. This suggests that the Areg survival factor could limit gefitinib toxicity by increasing BAX/Ku70 aggregate formation.

This hypothesis is sustained by our results with another NSCLC cell line H322, which does not secrete Areg.¹⁶ We showed that in H322, BAX/Ku70 interaction was not enhanced in the presence of gefitinib (Figure 3c). Adjunction of recombinant Areg in the culture medium slightly, but reproducibly, increased the sequestration of BAX by Ku70.

Areg inhibits the acetylation of Ku70

The interaction between BAX and Ku70 is regulated by acetylation. To further assess the effect of Areg on the state of Ku70 acetylation, we immunoprecipitated cytoplasmic Ku70 in H358 cells. After a treatment with gefitinib, the acetylation level of cytoplasmic Ku70 was below detection levels in our control conditions (Figure 3b, upper panel). However and as previously observed in Figure 3a, the gefitinib treatment enhanced the interaction between BAX and Ku70. This was demonstrated after reprob-ing the same blot with the anti-BAX antibody (bottom panel). In contrast, acetylation of Ku70 was markedly increased and detectable when H358 cells were treated with gefitinib and anti-

Areg siRNAs (upper panel). As expected, this hyperacetylation of Ku70 prevented BAX-Ku70 interaction, because we observed no detectable signal after BAX immunostaining (bottom panel). These results provide strong evidence that Areg inhibits the gefitinib-mediated acetylation of Ku70 and therefore enhances the sequestration of BAX by Ku70.

Ku70 acetylation increases the sensitivity of NSCLC cells to gefitinib

In vivo acetylation of proteins results from a subtle equilibrium between the opposite activities of acetyltransferases and deacetylases. Ku70 is known to be acetylated by HAT such as CREB-binding protein (CBP), p300 and p300/CBP-associated factor, whereas it can be deacetylated by both classes I/II HDAC and class III/sirtuin deacetylases.¹¹ To assess the involvement of acetylation, we first examined gefitinib-induced apoptosis in H358 cells overexpressing CBP. Overexpression of CBP had no significant effect per se, but sharply increased the amount of apoptosis in gefitinib-treated H358 cells as compared to control-transfected cells (Figure 4a).

H358 cells were then treated with several HDAC inhibitors. Although concentrations of up to 200 ng/ml trichostatin A (TSA, classes I/II HDAC inhibitor) alone did not significantly induce apoptosis, its combination with gefitinib showed a very significant and dose-dependent induction of apoptosis (Figure 4b). Gefitinib, in the presence of 200 ng/ml TSA, was ten times more toxic than when used alone. Similarly, suberoyl-anilide hydroxamic acid (vorinostat, classes I/II HDAC inhibitor,

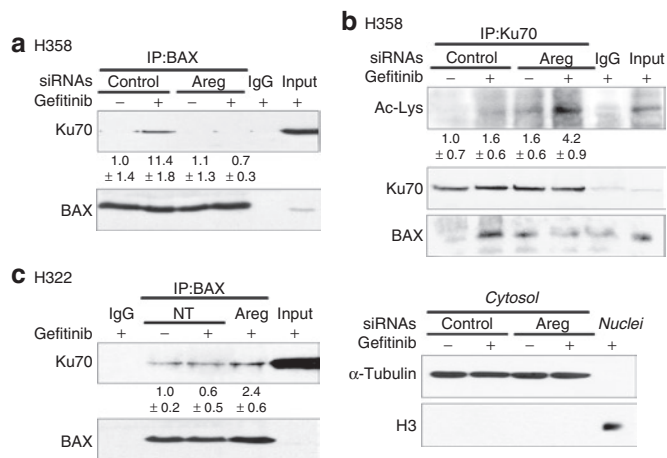


Figure 3 Areg enhances BAX-Ku70 interaction and inhibits Ku70 acetylation. (a,b) H358 cells were transfected with control or amphiregulin (Areg) small-interfering RNAs and 0.5 μmol/l gefitinib was applied as indicated for 96 hours. (c) H322 cells were treated or not with 50 ng/ml Areg and 0.5 μmol/l gefitinib for 96 hours as indicated. (a,c) Endogenous BAX immunoprecipitation (IP) was performed from whole-cell extracts and subjected to immunoblotting with Ku70 and BAX antibodies. The values denote the relative intensity of Ku70 protein bands of treated samples to that of control cells, after being normalized to the respective BAX and represent the average ± SD of independent experiments (H358 *n* = 3; H322 *n* = 2). (b) Endogenous Ku70 IP was performed from cytosolic extracts and subjected to immunoblotting with antiacetylated proteins and BAX antibodies. The immunoblot was reprobbed with Ku70 antibody to confirm the presence of an overlapping Ku70 band. The values denote the relative intensity of acetylated Ku70 bands of treated samples to that of control cells, after being normalized to the respective Ku70 and represent the average ± SD of three independent experiments. Cytosolic α-tubulin and nuclear histone H3 were used to show that cytoplasmic extracts were nuclear-free. IgG: irrelevant immunoglobulins, used as negative control. Inputs: cell lysates not subjected to immunoprecipitation, NT, non treated.

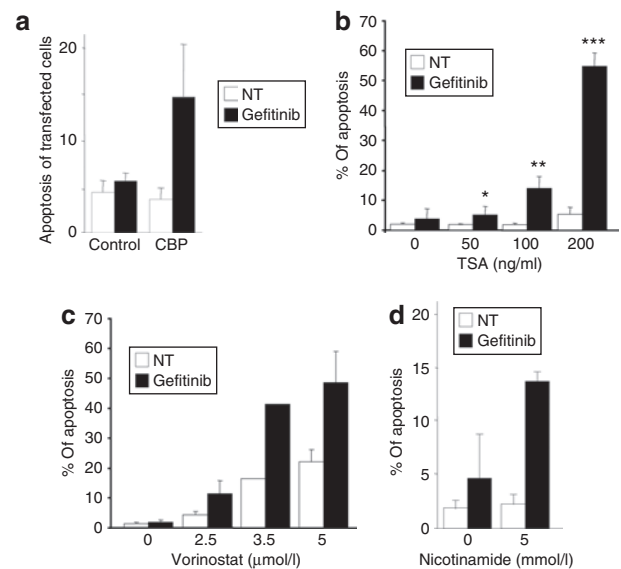


Figure 4 Enhanced Ku70 acetylation sensitizes H358 cells to gefitinib. (a) H358 cells were transfected with a plasmid control encoding green fluorescent protein (GFP) or with a plasmid encoding CREB-binding protein-hemagglutinin (CBP-HA) and treated or not with 0.5 μmol/l gefitinib as indicated. The expression of GFP or CBP-HA was revealed by immunofluorescence 96 hours after transfection and apoptosis of transfected cells was analyzed after counting Hoechst-stained cells. (b-d) H358 cells were treated or not with (b) TSA, (c) vorinostat, (d) nicotinamide, and/or 0.5 μmol/l gefitinib. Apoptosis was scored after counting Hoechst-stained cells. Results are expressed as mean ± SD (*n* ≥ 3). **P* < 0.05, ***P* < 0.01, ****P* < 0.001, more significant than control, NT, untreated.

Figure 4c) or nicotinamide (class III/sirtuin deacetylases inhibitor, Figure 4d) increased gefitinib-induced apoptosis. There was no significant effect of vorinostat or nicotinamide alone. These results suggest that an increased acetylation by HAT overexpression or HDAC inhibition sensitizes the cells to gefitinib.

TSA increases the gefitinib-mediated acetylation of Ku70

We then investigated whether increasing acetylation affected the gefitinib-mediated BAX-Ku70 interaction. The effect of TSA on cytoplasmic Ku70 was studied. TSA increased the acetylation of cytoplasmic Ku70 in gefitinib-treated cells (Figure 5a, upper panel). As expected, this increased acetylation of Ku70 was associated with a reduction of the BAX-Ku70 interaction (Figure 5a, middle panel). These results suggested that TSA sensitizes the cells to gefitinib's effect by enhancing Ku70 acetylation, leading to the subsequent release of BAX.

To consolidate this result, we constructed a K539R/K542R Ku70 mutant. Both lysines are known targets for acetylation, and govern BAX binding to Ku70. Their substitution by arginine amino acids prevents Ku70 acetylation.^{11,18,19} A control (empty plasmid), or plasmids encoding for wild-type or Ku70 mutant

proteins, were cotransfected in H358 cells and the level of apoptosis in the transfected cells was measured. As expected, 0.5 $\mu\text{mol/l}$ gefitinib or 200 ng/ml TSA alone did not induce significant apoptosis in any of the transfected cells (Figure 5b). The combined gefitinib and TSA treatments induced 50% apoptosis in control- or Ku70 wild-type-transfected cells, whereas only 30% of the cells transfected with the mutant form of Ku70 were apoptotic ($P < 0.05$) (Figure 5b). This experiment demonstrated that both lysines 539 and 542, necessary to the BAX-Ku70 interaction and Ku70 acetylation,¹⁸ are crucial for apoptosis induced by gefitinib and TSA cotreatment.

Antitumor efficacy of dual targeting HDAC and EGFR *in vivo*

Results presented in Figures 4 and 5 suggest that HDAC inhibitors counteract the protective effect of Areg and sensitize cells to gefitinib. To determine whether HDAC inhibitors are able to enhance the antitumor activity of gefitinib *in vivo*, we tested the effects of gefitinib, vorinostat, and their combination on the growth of H358 NSCLC xenograft tumors established in nude mice. Mice treated with a low concentration of gefitinib or vorinostat alone did not show reduced tumor growth as compared to control mice (Figure 6a). Mice treated with gefitinib and vorinostat combination treatment showed a strong inhibition of tumor growth as compared to control mice or to mice treated with gefitinib or vorinostat alone (Table 1). At the end of the study, the mean tumor volume in the combined-treatment group was 36% ($P < 0.01$) of the mean volume in the control group. No major modification on the level of acetylation under vorinostat treatment was observed using an antiacetylated histone H3K9 antibody or an antiacetylated proteins antibody on total proteins extracts and western blot analysis (data not shown) or after immunolabeling of tumor sections at the end of this experiment (Figure 6b, upper panel). In tumors from control mice or from mice treated with vorinostat or gefitinib alone, >40% of tumor cells are actively proliferating and thus expressed elevated levels of the Ki67 nuclear protein, whereas only 16% of the cells were cycling in the combined-treatment group ($P = 0.0039$, Figure 6b, lower panel and histogram). Gefitinib, vorinostat or the combination of both treatments were associated with increased levels of cleaved-caspase-3 in the tumors (Figure 6c). These findings suggest that the combined treatment enhanced the antitumor activity of each drug *in vivo* by reducing the proliferation of tumor cells. The combination of both molecules does not increase the level of apoptosis observed with each treatment separately. Taken together, these results indicate that the antitumor activity of gefitinib is enhanced when vorinostat is also present.

DISCUSSION

In the presence of Areg, NSCLC cells resist apoptosis induced by EGFR-TKI treatment such as gefitinib through BAX inactivation.⁹ In this study, we demonstrate that this effect is due to an acetylation-dependent mechanism leading to BAX sequestration by Ku70. We suggest a therapeutic approach to restore the EGFR-TKI sensitivity *in vitro* and *in vivo*.

We previously established that Areg inhibits BAX conformational activation and thus its translocation from the cytosol to the mitochondria in NSCLC cells.⁸ Several groups have shown

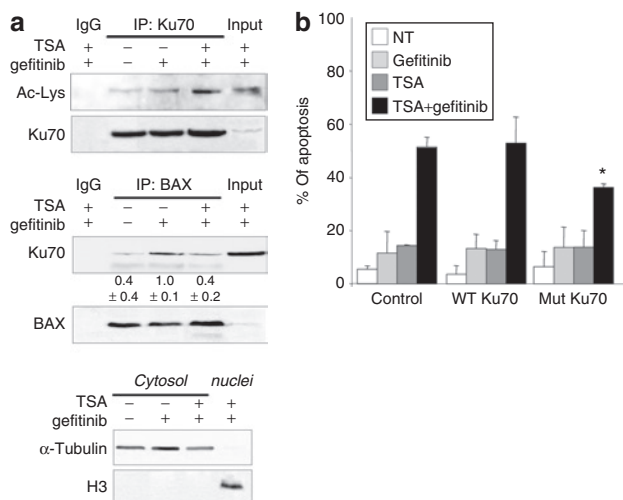


Figure 5 TSA-induced Ku70 acetylation regulates gefitinib-mediated apoptosis. (a) H358 cells were treated with 0.5 $\mu\text{mol/l}$ gefitinib and/or 200 ng/ml trichostatin A (TSA). Endogenous Ku70 immunoprecipitation (upper panel) was performed from cytosolic extracts and subjected to immunoblotting with antiacetylated proteins antibody. The immunoblot was reprobed with Ku70 antibody to confirm the presence of an overlapping Ku70 band. Endogenous BAX immunoprecipitation (middle panel) was performed from whole-cell extracts and subjected to immunoblotting with Ku70 and BAX antibodies. The values denote the relative intensity of Ku70 protein bands of treated samples to that of control cells, after being normalized to the respective BAX and represent the average \pm SD of three independent experiments. Cytosolic α -tubulin and nuclear histone H3 were used to show that cytoplasmic extracts were nuclear-free (lower panel). IgG: irrelevant immunoglobulins. Inputs: cell lysates not subjected to immunoprecipitation. (b) H358 cells were cotransfected with pEGFP-C1 and with control-pBJ5 or pBJ5-Ku70 wild-type or pBJ5-Ku70 K539R/K542R expression plasmids. Gefitinib 0.5 $\mu\text{mol/l}$ and/or TSA 200 ng/ml were added for 96 hours. Apoptosis was determined after Hoechst staining and counting apoptotic cells per 100 GFP-positive cells. Results are expressed as mean \pm SD ($n = 3$). * $P < 0.05$, less significant than control, NT, untreated.

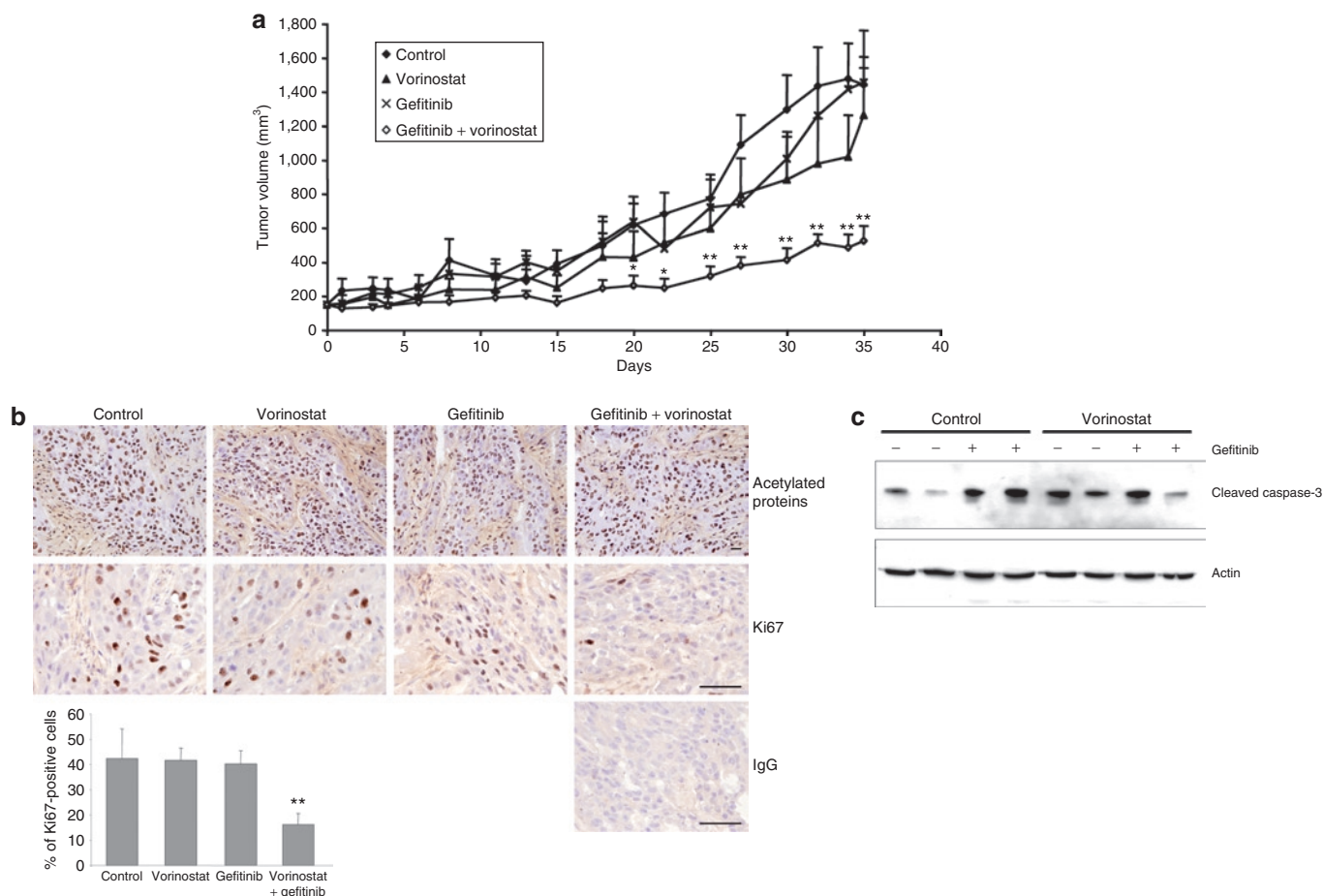


Figure 6 Antitumoral activity of gefitinib and HDAC inhibitor combined treatment *in vivo*. **(a)** Effects of combined treatment with gefitinib and vorinostat on growth of H358 xenograft tumors in athymic nude mice. The mice were randomly assigned to one of four treatment groups. Group 1 (control mice) received vehicle, group 2 received gefitinib, group 3 received vorinostat, and group 4 received gefitinib and vorinostat. Gefitinib (5 mg/kg body weight) or vorinostat (100 mg/kg body weight) were administered orally 5 days/week. Tumor volumes were measured 3 times a week. Points, mean tumor volume ($n = 8$); bars, SE. * $P < 0.05$, ** $P < 0.01$, for comparisons between treated and control for each series of experiments. **(b)** Acetylated proteins and Ki67 nuclear protein detected by immunostaining on frozen tumor sections from control mice, mice treated with vorinostat, gefitinib or both gefitinib and vorinostat, as indicated. IgG, irrelevant antibody. Bars = 50 μm . Histogram: the percentage of positive cells for Ki67 was determined after counting stained cells per 1,000 cells on a section. Results are expressed as mean \pm SD ($n = 6$ mice per group); ** $P = 0.0039$ for comparisons between combined treatment and control or single treatment. **(c)** Effect of gefitinib and vorinostat on the expression of activated-caspase-3 in H358 xenograft tumors, assessed by western blotting. Actin was used as loading control.

Table 1 Synergistic indexes of combination treatment of gefitinib and vorinostat

| Drug | Control | Vorinostat (treatment A) | Gefitinib (treatment B) | Vorinostat + gefitinib |
|--|-----------------|--------------------------|-------------------------|---|
| Mean volume (mm ³ \pm SE) | 1,442 \pm 513 | 1,262 \pm 786 | 1,454 \pm 869 | 524 \pm 243 |
| MGI ^a | 1 | 0.88 | 1.01 | 0.89 ^b 0.36 ^c 2.47 ^d |
| <i>P</i> value ^e | — | 0.468 | 0.663 | 0.0029 |

Growth inhibition rate on established subcutaneous tumor nodules in athymic nude mice treated with indicated concentrations of vorinostat, gefitinib or their combinations.

^aMean growth inhibition rate (MGI) = growth rate of treated group/growth rate of untreated group. ^bExpected MGI: growth inhibition rate of treatment A \times growth inhibition rate of treatment B. ^cObserved MGI: growth inhibition rate of combined treatment on treatments A and B. ^dIndex: calculated by dividing the expected growth inhibition rate by the observed growth inhibition rate. An index over 1 indicates synergistic effect and less than 1 indicates less than additive effect. ^e*P* value was calculated by *t*-test compared to control treatment.

the involvement of Ku70 in BAX inactivation in various pathologies such as neuroblastoma,¹⁸ leukemic cells,²⁰ genotoxic stress response,²¹ or imatinib resistance.^{22,23} Here, we demonstrate that Ku70 binds to and inhibits BAX activation in NSCLC cells in response to gefitinib.

In addition, we show that the Areg-mediated inactivation of BAX in the cytosol is the consequence of the inhibition of Ku70 acetylation (Figure 3). Accordingly, the knock down of Areg enhances gefitinib-induced Ku70 acetylation, leading to BAX release in its active, proapoptotic form. This important result suggests that Areg could play pivotal regulatory functions by influencing the acetylation of intracellular proteins.

Acetylation is emerging as an important mechanism by which many nonhistone proteins are regulated.^{24,25} Cell stress causes CBP- and/or p300/CBP-associated factor-dependent Ku70 acetylation. In addition, we proved that HDAC inhibitors such

as TSA can increase Ku70 acetylation. In both case, this acetylation of Ku70 is leading to the release of the proapoptotic form of BAX,¹⁵ which can translocate to the mitochondria, destabilize it and induce apoptosis.^{11,18,20,23} We also observed that overexpression of CBP or a TSA treatment in H358 cells sharply increased gefitinib-induced apoptosis. In our model, HDAC inhibitors such as TSA increased Ku70 acetylation and inhibited the BAX-Ku70 interaction, sensitizing H358 cells to gefitinib-induced apoptosis. These data demonstrated the involvement of both acetylases and deacetylases in Areg-dependent gefitinib-induced apoptosis regulation. These results also indicate that disruption of HAT-HDAC equilibrium governs nonhistone protein acetylation such as Ku70, thereby affecting Areg-dependent gefitinib resistance.

Ku70 is targeted for deacetylation by both class I/II HDAC and class III/sirtuin deacetylases.^{11,18,26} Accordingly, we observed an increased sensitivity to gefitinib under TSA, vorinostat and nicotinamide treatments. Thus, classes I/II and class III/sirtuin deacetylases participate in the regulation of Areg-induced resistance to apoptosis by regulating Ku70 acetylation. Interestingly, class IIB HDAC is involved in lung carcinogenesis.²⁷ Further experiments are needed to clearly identify which HDAC can be involved in this mechanism.

Our results suggested that HDAC inhibitors counteract the protective effect of Areg and sensitize cells to gefitinib by increasing the level of acetylated Ku70, thus inducing the release of active BAX from Ku70. This key result encourages the use of HDAC inhibitors as anticancer agents.²⁸ Indeed, HDACs are involved in several human cancers.²⁹ HDAC inhibitors were developed for cancer therapy and vorinostat was approved for treatment of cutaneous T cell lymphoma in 2006.³⁰ Recently, the HDAC inhibitor romidepsin has been shown to enhance the antitumor effect of EGFR-TKI erlotinib in NSCLC cell lines.³¹ We investigated an *in vivo* study combining HDAC inhibitors and EGFR-TKI on mice bearing NSCLC tumors. For the first time to our knowledge, a oral combination of vorinostat and gefitinib showed a major effect on inhibition of tumor growth. In tumors extracted 35 days after the beginning of treatment, vorinostat and gefitinib combined treatment induced an important and additive cell growth arrest. In addition, the cumulative effect of the dual treatment on apoptosis was obvious *in vitro* but was not significantly more elevated *in vivo*.

The sub-optimal doses of gefitinib and vorinostat, determined in preliminary experiments (data not shown), are not associated with any documented side-effect, and no sign of toxicity was observed in the cotreated animals. Possible effect of vorinostat on the average level of protein acetylation in the tumor extracts after completion of the treatment was not detected by western blot or immunohistochemistry. This is in agreement with other studies, which also failed to establish a correlation between the acetylation status and the tumor response.³² This result strongly supports the value of associating HDAC inhibitors and EGFR-TKI in NSCLC treatment, especially for EGFR-TKI-resistant patients. The molecular pathways activated *in vivo* by this combination of treatments, and especially the role of Ku70, still remain to be formally established.

In summary, our findings provide evidence that Areg mediates gefitinib resistance in NSCLC cells through an original acetylation-dependent pathway. Areg reduces Ku70 acetylation,

therefore strengthening the functional inhibition of BAX. This results in the inhibition of gefitinib toxicity in NSCLC cells. The involvement of acetylation mechanisms in gefitinib sensitivity should encourage the application of HDAC inhibitors as anticancer agents or in combination with EGFR-TKI treatments, especially in EGFR-TKI-resistant patients. Further studies are needed to validate whether the gefitinib treatment combined with HDAC inhibition could enhance the objective response and survival rates in NSCLC patients. Moreover, we demonstrated the therapeutic potential of Areg siRNAs combined with gefitinib treatment in NSCLC.⁹ It could be interesting to combine a specific anti-Areg siRNAs treatment with gefitinib, in order to augment its therapeutic benefit.⁹

MATERIALS AND METHODS

Cell culture and drug treatments. The human H358 and H322 NSCLC cell lines were from the American Type Culture Collection (Manassas, VA) and maintained in RPMI 1640 medium (Gibco, Cergy Pontoise, France) supplemented with 10% heat-inactivated fetal bovine serum in a humidified atmosphere with 5% CO₂. Gefitinib was kindly provided by AstraZeneca France (Paris, France) and was prepared as 10 mmol/l stock solution in dimethyl sulfoxide and stored at -20°C. Recombinant human Areg was from Sigma-Aldrich (St Quentin Fallavier, France) and stored at -80°C in dimethyl sulfoxide and dissolved in fresh medium just before use. TSA was from Sigma-Aldrich and prepared as 25 µg/ml stock solution, nicotinamide was from Sigma-Aldrich and prepared as 1 mol/l stock solution, and suberoylanilide hydroxamic acid or vorinostat was from Indofine Chemical Soc, (Hillsborough, NJ), prepared as 10 mmol/l stock solution and stored at -20°C. Cells were treated as indicated in figures legends.

Transfections. siRNAs targeting human Areg, human Ku70 and nonspecific control siRNAs were synthesized by MWG Biotech (Roissy, France). Sequences of siRNAs targeting Areg were 5'-CGA-ACC-ACA-AAU-ACC-UGG-CTT-3' and 5'-CCU-GGA-AGC-AGU-AAC-AUG-CTT-3'. Sequences of siRNAs targeting Ku70 were 5'-GAU-GCC-CUU-UAC-UGA-AAA-ATT-3' and 5'-UUC-UCU-UGG-UAA-CUU-UCC-CTT-3' and control siRNA sequence was 5'-CUU-ACG-CUC-ACU-ACU-GCG-ATT-3'. Transfection of duplex siRNAs was performed with Oligofectamine reagent (Invitrogen, Cergy Pontoise, France), following the manufacturer's instructions. SiRNAs were transfected into 60% confluent cells at the final concentration of 200 nmol/l. After transfection, the efficiency of Areg knockdown was assessed by enzyme-linked immunosorbent assay as previously described¹⁶ and the efficiency of Ku70 knockdown was assessed by western blotting.

Transient transfections were carried out on H358 cells cultured on Lab-Tek two wells. Cells were transfected using Eugene (Roche Diagnostics, Meylan, France) according to the manufacturer's protocol, with 1.5 µg of an expression vector encoding CBP-hemagglutinin or a control vector encoding green fluorescent protein (GFP). H358 cells were also transfected with control-pBJ5 or pBJ5-Ku70 wild-type (provided by D. Trouche) or pBJ5-Ku70 K539R/K542R (generated using a QuickChange site-directed mutagenesis kit, Stratagene), along with pEGFP-C1 expression vector (Clontech, St Germain en Laye, France), using JetPEI (PolyPlus Transfection, Strasbourg, France) and according manufacturer's instructions. Immunofluorescence was performed 96 hours after transfection.

Apoptosis assays. Cells were harvested and pooled. The morphological changes related to apoptosis were assessed by fluorescence microscopy after Hoechst 33342 (5 µg/ml, Sigma-Aldrich) staining of cells and the percent of apoptotic cells was scored after counting at least 500 cells. Active caspase-3 was detected by flow cytometry using phycoerythrin-conjugated

monoclonal active caspase-3 antibody kit (BD Pharmingen, Pont de Claix, France), following manufacturer's instructions. Analysis was performed on a Becton Dickinson FACScan flow cytometer with CellQuest Software (Becton Dickinson, Pont de Claix, France).

Protein immunostaining by flow cytometry. Activated-BAX immunostaining analysis was performed as previously described.^{8,33} Briefly, fixed cells were first incubated with anti-activated-BAX antibody (N-20, 1:100; Santa Cruz Biotechnology, Tebu, France) or with irrelevant immunoglobulin G (IgG) (BD Pharmingen). Then washed cells were incubated with Alexa 488 anti-rabbit IgG (H+L) conjugate (1:1,000; Interchim, Montluçon, France). Analysis was performed on a FACScan flow cytometer (Becton Dickinson) using Cellquest software. Green fluorescence was excited at 488 nm and detected at 500–550 nm.

Immunofluorescence staining. Cells cultured on Lab-Tek were transfected as indicated. 96 hours after transfection, fixed cells were incubated with anti-hemagglutinin.11 (1:1,000; Covance, Eurogentec). Second incubation was performed with Alexa 488 goat anti-rabbit IgG (H+L) conjugate (1:500; Interchim, Montluçon, France). Cells were then counterstained with Hoechst 33342 and observed using an Olympus microscope.

Subcellular fractionation and protein extraction. Total cell lysates were obtained after washing cells twice in phosphate-buffered saline and incubated in radioimmuno precipitation assay lysis buffer (Tris-HCl 50 mmol/l pH 7.4, NaCl 150 mmol/l, Nonidet P-40 1%, sodium deoxycholate 0.5%, sodium dodecyl sulfate 0.1%) with proteases and phosphatases inhibitors (NaF 1 mmol/l, Na₃VO₄ 1 mmol/l, PMSF 0.5 mmol/l, leupeptin 10 µg/ml, aprotinin 10 µg/ml and pepstatin 10 µg/ml) for 30 minutes on ice.

Cytosolic extracts for acetylation experiments were obtained as follows: cells were incubated with 50 ng/ml TSA overnight before 15 minutes incubation in hypotonic buffer (100 ng/ml TSA, Tris-HCl pH 7.5 10 mmol/l, KCl 10 mmol/l, MgCl₂ 1.5 mmol/l, DTT 0.5 mmol/l) with protease and phosphatase inhibitors. Cells were then incubated 10 minutes with hypotonic buffer supplemented with NP40 1%. The supernatant contained the cytoplasmic proteins.

Fractions extracts were assessed for protein content using the Bio-Rad D C Protein Assay kit, and 20 µg of proteins were subjected to electrophoresis and analyzed by western blotting for BAX and Ku70 content. The relative purity of fractions was ascertained by western blotting using α -tubulin (Sigma-Aldrich) as a marker of cytosol and histone H3 (Upstate, Molsheim, France) as a marker of nucleus.

Immunoblotting and coimmunoprecipitation. Endogenous BAX immunoprecipitations were performed using 1 mg protein from whole-cell extracts and 1 µg BAX antibody (BD Pharmingen) or irrelevant rabbit IgG for negative control and by incubating overnight at 4°C under gentle agitation. Cytosolic Ku70 immunoprecipitations were done using 4 mg protein and 1 µg Ku70 antibody (Santa Cruz Biotechnology) or irrelevant mouse IgG_{2b} for negative control and by incubating overnight at 4°C under agitation. The immunocomplexes were collected using protein-G agarose (Sigma-Aldrich). The immunoprecipitates were resolved on sodium dodecyl sulfate–polyacrylamide gel electrophoresis gels, followed by western blotting with acetylated protein (1/1,000; Abcam, Paris, France), Ku70 (1/1,000; Santa Cruz Biotechnology) or BAX (1/3,000; BD Pharmingen) antibodies. The immunoblot for acetylated protein was re-probed with Ku70 antibody to confirm the presence of an overlapping Ku70 band.

Western blotting was also done using anticlaved caspase-3 (1/1,000; Asp 175, Cell Signaling, St Quentin en Yvelines, France) antibodies. To ensure equal loading and transfer, membranes were also probed for actin using antiactin antibody (Sigma, 1/1,000). Western blotting was further processed by standard procedures and revealed by chemiluminescence (ECL; Amersham, Orsay, France).

The relative intensity, measured using ImageJ (NIH software), of acetylated Ku70 bands or total Ku70 of treated samples to that of control cells was normalized to the respective Ku70 or BAX, respectively.

In vivo model. The effect of the combination of gefitinib and vorinostat was measured on established subcutaneous tumor bearing mice. All the animal experiments were performed in agreement with the European Economic Community guidelines and the “Principles of laboratory animal care” (NIH publication N 86-23 revised 1985). The experimental protocol was submitted to ethical evaluation and the experiment received the accreditation number 0260. Human lung adenocarcinoma H358 cells were harvested from culture, and 20 × 10⁶ cells in sterile phosphate-buffered saline were injected subcutaneously into the flank of female NMRI nude mice (6–8 weeks old, Janvier, Le Genest Saint Isle, France). When tumor diameters reached 5 mm, mice were randomized in four experimental groups (10 mice/group). Group 1 (control mice) received a vehicle (tween/glucose), group 2 received vorinostat, group 3 received gefitinib, and group 4 received both vorinostat and gefitinib. Five mg/kg/day of gefitinib and/or 100 mg/kg/day of vorinostat were administered orally in tween/glucose, 5 days a week. Tumor growth was quantified by measuring twice a week the tumors in two dimensions with a Vernier caliper. The volume was calculated as follows: $a \times b^2 \times 0.4$, where a and b are the largest and smallest diameters, respectively. Results are expressed as volume ± SEM. Mice bearing necrotic tumors or tumors ≥1.5 cm in diameter were euthanized immediately. On day 36, all mice were killed and tumors were collected before further analyses by western blotting and immunohistochemistry.

Immunohistochemical staining. Tumor sections of 7 µm thickness were fixed with 3.7% paraformaldehyde for 10 minutes at room temperature, then saturated for 5 minutes with 0.03% bovine serum albumin, incubated overnight at 4°C with rabbit antiacetylated lysine antibody (1/200; Cell Signaling) or with monoclonal mouse antihuman Ki67 (1/150; Dako, Trappes, France). Immunohistochemistry was further processed using the Histostain-Plus Bulk Kit (Invitrogen). The final reaction product was visualized with diaminobenzidine. After immunohistochemical reactions, sections were counterstained with hematoxylin. Negative controls were performed with the same sections incubated with irrelevant antibody (rabbit IgG 1/40,000 or mouse IgG 1/30,000).

Statistical analyses. Statistical significance of difference in treatment was analyzed by Mann–Whitney test. Means comparisons among groups and statistical significance of differences in tumor growth in the combination treatment group and in single-agent treatment groups were analyzed by ANOVA test. Statistics were done using Statview 4.1 software (Abacus Concept, Berkeley, CA). In all statistical analyses, two-sided P values < 0.05 were considered statistically significant.

ACKNOWLEDGMENTS

We thank AstraZeneca for gefitinib, D. Trouche (CNRS UMR5088, France) for Ku70 wild-type expression vector, Laetitia VanWanterghem and Corine Tenaud for technical assistance. This work was supported by grants and research fellowship from La Ligue contre le Cancer, comité de la Drôme; EpiPro program (InCa) and “projet libre INCa”, PL06_025, to MCF and SK laboratories; ARECA program (ARC) to SK laboratory and with the help of a “subvention-libre” from the ARC (Association pour la Recherche sur le Cancer).

REFERENCES

- Garcia de Palazzo, IE, Adams, GP, Sundareshan, P, Wong, AJ, Testa, JR, Bigner, DD *et al.* (1993). Expression of mutated epidermal growth factor receptor by non-small cell lung carcinomas. *Cancer Res* **53**: 3217–3220.
- Rusch, V, Baselga, J, Cordon-Cardo, C, Orazem, J, Zaman, M, Hoda, S *et al.* (1993). Differential expression of the epidermal growth factor receptor and its ligands in primary non-small cell lung cancers and adjacent benign lung. *Cancer Res* **53**(10 Suppl): 2379–2385.
- Fukuoka, M, Yano, S, Giaccone, G, Tamura, T, Nakagawa, K, Douillard, JY *et al.* (2003). Multi-institutional randomized phase II trial of gefitinib for previously treated patients with advanced non-small-cell lung cancer (The IDEAL 1 Trial) [corrected]. *J Clin Oncol* **21**: 2237–2246.
- Shepherd, FA, Rodrigues Pereira, J, Ciuleanu, T, Tan, EH, Hirsh, V, Thongprasert, S *et al.*; National Cancer Institute of Canada Clinical Trials Group (2005). Erlotinib in previously treated non-small-cell lung cancer. *N Engl J Med* **353**: 123–132.

5. Thatcher, N, Chang, A, Parikh, P, Rodrigues Pereira, J, Ciuleanu, T, von Pawel, J *et al.* (2005). Gefitinib plus best supportive care in previously treated patients with refractory advanced non-small-cell lung cancer: results from a randomised, placebo-controlled, multicentre study (Iressa Survival Evaluation in Lung Cancer). *Lancet* **366**: 1527–1537.
6. Ishikawa, N, Daigo, Y, Takano, A, Taniwaki, M, Kato, T, Hayama, S *et al.* (2005). Increases of amphiregulin and transforming growth factor- α in serum as predictors of poor response to gefitinib among patients with advanced non-small cell lung cancers. *Cancer Res* **65**: 9176–9184.
7. Busser, B, Coll, JL and Hurbini, A (2008). The increasing role of amphiregulin in non-small cell lung cancer. *Pathol Biol* (epub ahead of print).
8. Hurbini, A, Coll, JL, Dubrez-Daloz, L, Mari, B, Auburger, P, Brambilla, C *et al.* (2005). Cooperation of amphiregulin and insulin-like growth factor-1 inhibits Bax- and Bad-mediated apoptosis via a protein kinase C-dependent pathway in non-small cell lung cancer cells. *J Biol Chem* **280**: 19757–19767.
9. Busser, B, Sancey, L, Josseland, V, Niang, C, Favrot, MC, Coll, J-L *et al.* Amphiregulin promotes BAX inhibition and resistance to gefitinib in non-small-cell lung cancers. *Mol Ther*, this issue.
10. Scorrano, L and Korsmeyer, SJ (2003). Mechanisms of cytochrome c release by proapoptotic BCL-2 family members. *Biochem Biophys Res Commun* **304**: 437–444.
11. Cohen, HY, Lavu, S, Bitterman, KJ, Hekking, B, Imahiyerobo, TA, Miller, C *et al.* (2004). Acetylation of the C terminus of Ku70 by CBP and PCAF controls Bax-mediated apoptosis. *Mol Cell* **13**: 627–638.
12. Gullo, C, Au, M, Feng, G and Teoh, G (2006). The biology of Ku and its potential oncogenic role in cancer. *Biochim Biophys Acta* **1765**: 223–234.
13. Featherstone, C and Jackson, SP (1999). Ku, a DNA repair protein with multiple cellular functions? *Mutat Res* **434**: 3–15.
14. Tuteja, R and Tuteja, N (2000). Ku autoantigen: a multifunctional DNA-binding protein. *Crit Rev Biochem Mol Biol* **35**: 1–33.
15. Witta, SE, Gemmill, RM, Hirsch, FR, Coldren, CD, Hedman, K, Ravdel, L *et al.* (2006). Restoring E-cadherin expression increases sensitivity to epidermal growth factor receptor inhibitors in lung cancer cell lines. *Cancer Res* **66**: 944–950.
16. Hurbini, A, Dubrez, L, Coll, JL and Favrot, MC (2002). Inhibition of apoptosis by amphiregulin via an insulin-like growth factor-1 receptor-dependent pathway in non-small cell lung cancer cell lines. *J Biol Chem* **277**: 49127–49133.
17. Desagher, S, Osen-Sand, A, Nichols, A, Eskes, R, Montessuit, S, Lauper, S *et al.* (1999). Bid-induced conformational change of Bax is responsible for mitochondrial cytochrome c release during apoptosis. *J Cell Biol* **144**: 891–901.
18. Subramanian, C, Oipari, AW Jr, Bian, X, Castle, VP and Kwok, RP (2005). Ku70 acetylation mediates neuroblastoma cell death induced by histone deacetylase inhibitors. *Proc Natl Acad Sci USA* **102**: 4842–4847.
19. Subramanian, C, Jarzembowski, JA, Oipari, AW Jr, Castle, VP and Kwok, RP (2007). CREB-binding protein is a mediator of neuroblastoma cell death induced by the histone deacetylase inhibitor trichostatin A. *Neoplasia* **9**: 495–503.
20. Sutheesophon, K, Kobayashi, Y, Takatoku, MA, Ozawa, K, Kano, Y, Ishii, H *et al.* (2006). Histone deacetylase inhibitor depsipeptide (FK228) induces apoptosis in leukemic cells by facilitating mitochondrial translocation of Bax, which is enhanced by the proteasome inhibitor bortezomib. *Acta Haematol* **115**: 78–90.
21. Mazumder, S, Plesca, D, Kinter, M and Almasan, A (2007). Interaction of a cyclin E fragment with Ku70 regulates Bax-mediated apoptosis. *Mol Cell Biol* **27**: 3511–3520.
22. Ju, DS, Kim, MJ, Bae, JH, Song, HS, Chung, BS, Lee, MK *et al.* (2007). Camptothecin acts synergistically with imatinib and overcomes imatinib resistance through Bcr-Abl independence in human K562 cells. *Cancer Lett* **252**: 75–85.
23. Lee, SM, Bae, JH, Kim, MJ, Lee, HS, Lee, MK, Chung, BS *et al.* (2007). Bcr-Abl-independent imatinib-resistant K562 cells show aberrant protein acetylation and increased sensitivity to histone deacetylase inhibitors. *J Pharmacol Exp Ther* **322**: 1084–1092.
24. Spange, S, Wagner, T, Heinzl, T and Krämer, OH (2009). Acetylation of non-histone proteins modulates cellular signalling at multiple levels. *Int J Biochem Cell Biol* **41**: 185–198.
25. Minucci, S and Pelicci, PG (2006). Histone deacetylase inhibitors and the promise of epigenetic (and more) treatments for cancer. *Nat Rev Cancer* **6**: 38–51.
26. Sundaresan, NR, Samant, SA, Pillai, VB, Rajamohan, SB and Gupta, MP (2008). SIRT3 is a stress-responsive deacetylase in cardiomyocytes that protects cells from stress-mediated cell death by deacetylation of Ku70. *Mol Cell Biol* **28**: 6384–6401.
27. Kamemura, K, Ito, A, Shimazu, T, Matsuyama, A, Maeda, S, Yao, TP *et al.* (2008). Effects of downregulated HDAC6 expression on the proliferation of lung cancer cells. *Biochem Biophys Res Commun* **374**: 84–89.
28. Bolden, JE, Peart, MJ and Johnstone, RW (2006). Anticancer activities of histone deacetylase inhibitors. *Nat Rev Drug Discov* **5**: 769–784.
29. Yang, XJ and Seto, E (2007). HATs and HDACs: from structure, function and regulation to novel strategies for therapy and prevention. *Oncogene* **26**: 5310–5318.
30. Grant, S, Easley, C and Kirkpatrick, P (2007). Vorinostat. *Nat Rev Drug Discov* **6**: 21–22.
31. Zhang, W, Peyton, M, Xie, Y, Soh, J, Minna, JD, Gazdar, AF *et al.* (2009). Histone deacetylase inhibitor romidepsin enhances anti-tumor effect of erlotinib in non-small cell lung cancer (NSCLC) cell lines. *J Thorac Oncol* **4**: 161–166.
32. Prince, HM, Bishton, MJ and Harrison, SJ (2009). Clinical studies of histone deacetylase inhibitors. *Clin Cancer Res* **15**: 3958–3969.
33. Dubrez, L, Coll, JL, Hurbini, A, Solary, E and Favrot, MC (2001). Caffeine sensitizes human H358 cell line to p53-mediated apoptosis by inducing mitochondrial translocation and conformational change of BAX protein. *J Biol Chem* **276**: 38980–38987.